Effect of lateral load on the pile's buckling instability in liquefied soil

Xiaoyu Zhang[1], Liang Tang[2], Xianzhang Ling[3] and Andrew H. C. Chan[4]

1. Corresponding Author. Ph. D. Candidate, School of Civil Engineering, Harbin Institute of Technology, Harbin, Heilongjiang 150090, China.
   Email: zxy_hit@163.com

2. Professor, School of Civil Engineering, Harbin Institute of Technology, Harbin, Heilongjiang 150090, China.
   Email: hit_tl@163.com

3. Professor, School of Civil Engineering, Harbin Institute of Technology, Harbin, Heilongjiang 150090, China.
   Email: xianzhang_ling@263.net

4. Professor, School of Engineering and ICT, University of Tasmania, Hobart, Tasmania 7001, Australia.
   Email: andrew.chan@utas.edu.au

Abstract

Even with modern design guidelines, the collapse of pile-supported structures in liquefiable deposits is still observed after strong earthquakes, and buckling instability of piles has been cited as a possible mechanism of failure in liquefiable soils. However, the effect of lateral load on buckling instability of the pile in liquefied soils has not been adequately investigated. This paper presents a shake-table test, which is conducted to study the failure mechanism of an end-bearing pile partly embedded in a saturated sand layer. It is found that pile with a large mass at the top failed in buckling after the soil fully liquefied. Then, a pseudo-static analysis method is proposed to evaluate the buckling instability of the pile under the combination of lateral and axial load. The buckling load of the pile was found to decrease with the increase in lateral inertial load. It is hence important for the designers to consider the level of lateral loading during buckling analysis of pile in liquefiable ground. Finally, a possible boundary for safe design is purposed to avoid buckling failure of the pile while considering the effect of inertial load.

Keywords: Liquefaction; Pile foundation; Buckling instability; Pseudo-static analysis; Shake-table test

1. Introduction

Many attempts have been made in recent decades to explore the seismic behavior of the pile foundation in liquefiable soils and various design guidelines have been formulated (Abdoun et al. 2003; Brandenberg et al. 2013). However, pile failures are still detected, for instance, the damage survey of pile supported structure in 1995 Kobe Earthquake, 2001 Bhuj Earthquake, and 2005 Sumatra Earthquake (Bhattacharya and Madabhushi 2008; Haldar et al. 2008). This is a sign that the understanding of the failure mechanisms of the pile in liquefying ground may not be adequate (Haldar et al. 2008).

The well-established theory of pile failure is based on a bending mechanism, where the pile is treated as a laterally loaded beam, and the lateral loads (due to inertia and/or lateral spreading) induce bending failure in a pile (Bhattacharya and Madabhushi 2008). This failure mechanism is generally regarded as the main reason for many pile foundations failure during earthquakes, such as Abdoun and Dobry (2002), Finn and Fujita (2002), and Tokimatsu et al. (1998). Recently, buckling instability has been cited as another possible mechanism of pile failure in liquefied soils (Bhattacharya et al. 2004; Knappett and Madabhushi 2009; Shanker et al. 2007). Bhattacharya (2003) demonstrated that when the soil around the pile loses much of its stiffness and strength due to liquefaction, the pile will become an unsupported long slender column and could buckle under the high axial load from the superstructure.

In fact, the failure mechanism of the pile in liquefied soils is different from the unsupported long slender column under axial load, because there is always some lateral loads acting on the pile. The lateral loads, due to inertia and lateral spreading, could increase the lateral deflection of the pile and thus reduce the axial load required for buckling (Bhattacharya and Madabhushi 2008). On the other hand, there will always be confining pressure around the pile even if the soil has fully liquefied, and it could provide some lateral support to the pile and increase the buckling load (i.e., the greatest axial load that will not cause buckling) (Bhattacharya et al. 2005). However, the existing studies concerning the buckling instability of pile in liquefied soils ignoring the effect of lateral loads. For instance, the inertial load was removed in the pile buckling failure centrifuge tests by Bhattacharya et al. (2004) and Knappett and Madabhushi (2009). Furthermore, the buckling load is calculated using the Euler buckling formula, in which the confining pressure around the pile is not considered, in Bhattacharya et al. (2004) and Haldar et al. (2008). Even though this will result in a lower buckling load, this is unnecessarily conservative. Only a limited studies have been carried out to discuss the effect of the combined action of lateral load and axial load on the pile failure in liquefied soils (Dash et al. 2010; Haldar et al. 2008), and these studies are mainly focused on the effect of axial load on the bending behavior of pile. In this paper, attention is concentrated on the influence of lateral loads on the buckling failure of a single fully embedded end-bearing pile passing through the liquefiable saturated sand.

In the following sections, the shake-table test is described first, with results analyzed. Then, a pseudo-static analysis method which is based on the Beam on Nonlinear Winkler Foundation (BNWF) model was adopted to simulate the pile response in liquefied soils. Next, the buckling instability of pile under the combined action of lateral load and axial load is studied using the developed pseudo-static analysis method. Finally, the conclusion remarks are drawn.

2. Description of the shake-table test

A shake-table test [Figs. 1 and 2(a)] on the failure mechanism of the pile in liquefying ground was performed. This shake-table test used a rectangular laminar soil container that was 3.5 m long, 2.0 m wide, and 1.7 m high (Chen et al. 2016).

The soil profile consisted of a horizontal saturated sand, the depth of which is 1.5 m thick (Fig. 1). Fine Nanjing sand was placed into the soil container, to form the horizontally homogeneous sand stratum using the water sedimentation method (Ishihara 1993). The water table was set at the ground surface. The relative density of the sand stratum was about 40-50%, and the saturated density of the sand was about 1,880 kg/m^3. The properties of sand are listed in Table 1 (Chen et al., 2016).

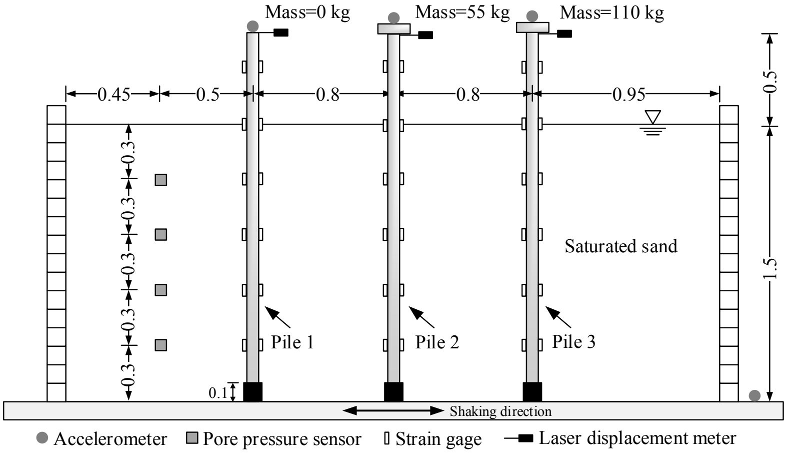

Fig. 1 Experimental setup (unit: m)

Three aluminum pipe piles (i.e., Piles 1, 2 and 3) with same properties were studied in the test (Fig. 1). The properties of the pile are tabulated in Table 2. Before the construction of the soil layer, the piles were connected to the base in an attempt to achieve a fixity boundary condition. To investigate the pile behavior under different inertial load and axial load, individual masses of 55 kg and 110 kg were applied on the top of Pile 2 and Pile 3, respectively. Moreover, no constraint is applied on the pile top to prevent the pile deformation within the soil.

Table 1 Properties of Nanjing sand

Parameters	Value
Specific gravity	2.70
Maximum void ratio, e_{max}	1.15
Minimum void ratio, e_{min}	0.62
Coefficient of curvature, C_c	1.07
Coefficient of uniformity, C_u	2.31
Mean grain size, D_{50} (mm)	0.13

Table 2 Pile properties

Parameters	Value
Pile length, L	1.9 m
Outside diameter, D	0.041 m
Wall thickness, t	1.1 mm
Young's modulus, E	6.9×10^4 MPa
Yield strength	276 MPa
Ultimate tensile strength	310 MPa

The shaking of the model was carried out along the longitudinal direction of the model (Fig. 1). The base excitation was a sinusoidal seismic input with the dominant frequency of 2 Hz and amplitude of approximately 0.21 g. Excess pore pressure within the sand and pile response: pile head acceleration, lateral displacement, and pile strain, were recorded.

3. Experimental results and analysis

In this section, the experimental results regarding the behavior of the soil and pile are presented and discussed.

Well-known evidence of soil liquefaction, sand boils, was observed at the ground surface during the shaking [Fig. 2(b)], which indicates that liquefaction had occurred in the saturated sand. The presence of liquefaction could also be reflected by the measured excess pore pressure (u_e), as shown in Fig. 3.

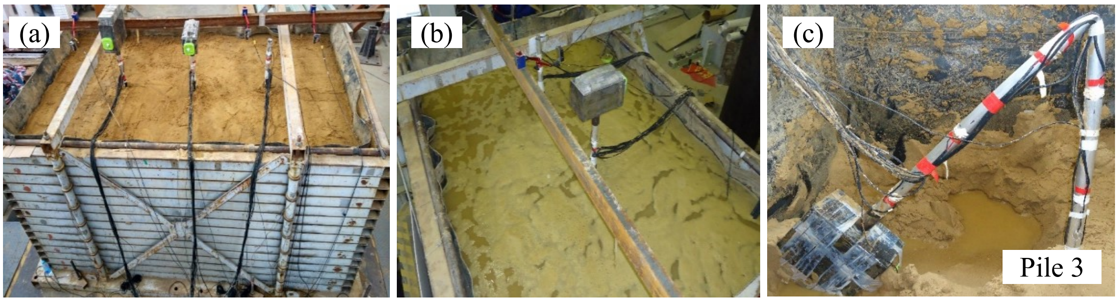

Fig. 2 Shake-table test: (a) before the test; (b) after the test; and (c) damage to Pile 3

Piles 1 and 2 were intact after the shaking, while Pile 3 was damaged during the shaking. Fig. 2(c) exhibit the damage pattern of Pile 3 after excavation. The collapse direction of the pile is almost orthogonal to the shaking direction. Fig. 4 shows the time history of the pile head lateral displacement recorded by the laser displacement meter. The maximum lateral displacement for Piles 1 and 2 were 27 mm and 56 mm, respectively. For Pile 3, due to its failure, only the lateral displacement at the initial 2 second could be recorded because the measured value by laser displacement meter is over the range, and the maximum lateral displacement is 51 mm at that point in time. It can be concluded that the moment of failure for Pile 3 is 2 sec after shaking started and it is the time that soil has just attained full liquefaction (Fig. 3).

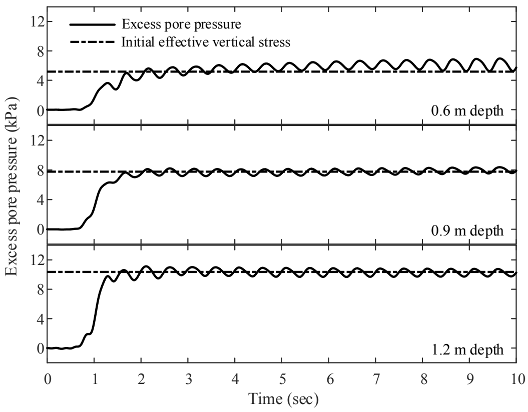

Fig. 3 Excess pore pressure time histories

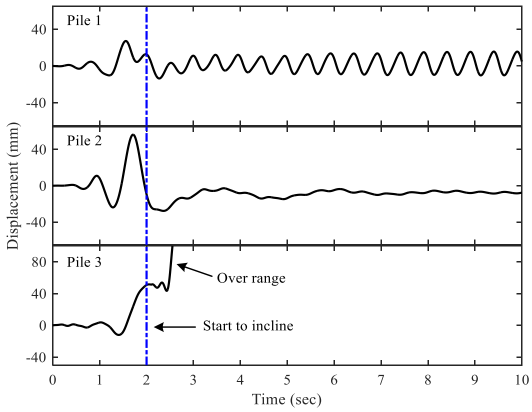

Fig. 4 Displacement time histories of pile head

Pile foundations in liquefiable soils under strong earthquake may fail due to excessive settlement, shear, bending, and buckling (Dash et al. 2010). For the damage of Pile 3, failure due to settlement is impossible because it is an end-bearing pile. Also, the shear failure is unlikely to happen in this case as the soil profile consisted of only one horizontal stratum of saturated sand. Thus, the reason of Pile 3 failure could be bending or buckling.

If the damage of Pile 3 is a bending failure, the damage could be mainly caused by the inertial force, as no lateral spreading was observed in this test. If the pile failed in a flexural mode, the direction of collapse should be same as that of the inertial load (i.e., along the shaking direction), whereas the observed direction of pile collapse is orthogonal to the shaking direction. Meanwhile, from the experimental results (Fig. 5), the maximum pile bending moment occurred either at pile bottom or ground surface, therefore, the possible position of the hinge should be at the bottom of the pile or soil surface. However, the position of the hinge for Pile 3 was found at 0.46 m depth (Fig. 5). Furthermore, the maximum tensile stress in Pile 3 was 42 MPa as calculated from the recorded strains, which is much less than the ultimate strength of 310 MPa. Therefore it can be concluded that bending failure was not the main cause of damage for Pile 3.

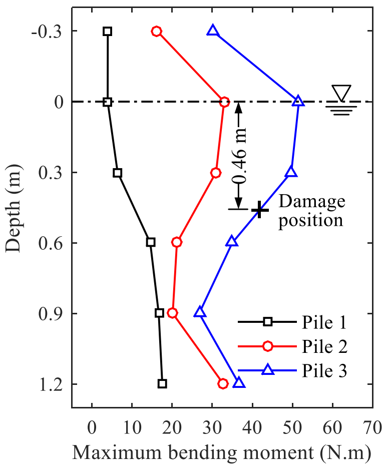

Fig. 5 Maximum pile bending moment profiles

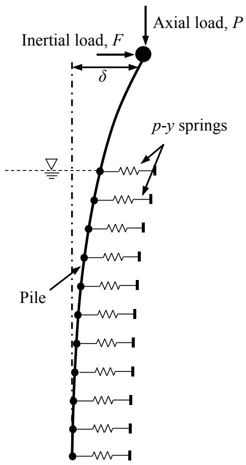

Fig. 6 Pseudo-static analysis of pile response

On the other hand, the pile which has a high slenderness ratio (above 50) is expected to fail in buckling instability (Bhattacharya et al. 2004). The slenderness ratio of Pile 3 which is calculated as suggested by Bhattacharya et al. (2004) is 283 which is much larger than 50. Moreover, as reported by Bhattacharya (2006), the possible buckling load is as long as 0.35 times of the theoretical Euler's buckling load (P_E), which is computed as follows,

$$P_E = \frac{\pi^2 EI}{L_{eff}^2} \tag{1}$$

where L_{eff} is the effective length of the pile and EI is the bending stiffness of the pile. Note that Pile 3 has an axial load of 1.08 kN which is 0.92 times P_E. Based upon the above analysis, the damage of Pile 3 could be categorized as the buckling instability.

4. Buckling instability of the pile under the combined action of lateral load and axial load

The buckling failure of Pile 3 could be caused not only by the larger axial load but also influenced by lateral load due to the inertia effect. To investigate the effect of lateral load on the buckling load of pile, a pseudo-static analysis method is presented in this section.

4.1 Finite element modeling

All finite element simulations were performed using the Open System for Earthquake Engineering Simulation, OpenSees (http://opensees.berkeley.edu, Mazzoni et al. 2006).

A pseudo-static analysis method which is based on the BNWF model was used to study the behavior of pile in liquefied soils (Fig. 6). The pile was simulated with elastic beam-column elements. The pile-soil interaction was modeled using discrete *p-y* springs for lateral loading using the PySimple1 uniaxial material model (Brandenberg et al. 2013; Turner et al. 2016). For the nonlinear *p-y* springs, ultimate resistance (p_{ult}), initial stiffness, and relative displacement between the pile and the soil with 50 percent of p_{ult} mobilized (y_{50}) were calculated from the values of friction angle and relative density, in this study the formulation developed by the American Petroleum Institute (API) was used. The influence of the liquefaction was considered by multiplying the computed p_{ult} by a degradation factor m_p which is widely known as *p-multiplier*, and the value of m_p= 0.1 was used for the full liquefaction condition (Boulanger et al. 2003).

The pile head was free to move, and the pile bottom was fully fixed which is employed to simulate the boundary condition of the end-bearing pile. A "P-Delta transformation" was used to considering second-order P-Delta effects (Mazzoni et al. 2006), which implies that all equilibrium equations are solved using the deformed configurations of the models. The finite-element analyses were employing the norm of the displacement increment (NormDispIncr command) to test for convergence with a tolerance of 1.0×10^{-6} m, while using a Newton-Raphson solution algorithm (Mazzoni et al. 2006).

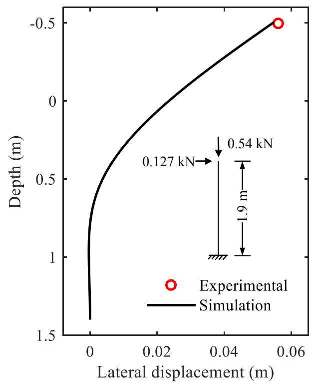

Fig. 7 Comparison of the experimental and computed lateral displacement of Pile 2

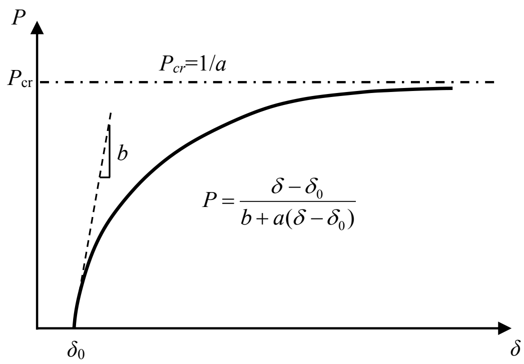

Fig. 8 The method of estimating buckling load (P_{cr})

The aforementioned pseudo-static analysis method has been validated and used for predicting the pile response in liquefiable soils by several researchers (Boulanger et al. 2003; Turner et al. 2016). To further ensure the validity of the numerical model, a pile analysis with the *p-y* springs was carried out to capture the response of Pile 2 at the moment of maximum pile head displacement (1.8 sec) in this shake-table test. An axial load of 0.54 kN (gravity load from superstructure) and a lateral load of 0.127 kN (i.e., inertial load, calculated using the recorded pile head acceleration) were acting at the pile head, and the pile properties are given in Table 2 (Fig. 7). The *p-y* curves with m_p= 0.1 were used to consider the pile-soil interaction, and the friction angle of sand used was also 31.6°. The computed pile lateral displacement is shown in Fig. 7 for comparison, a very good congruence is found between the experimental lateral displacement and the calculated results.

4.2 Method of estimating buckling load

The relationship between the pile head lateral deflection and axial load could be fitted using a hyperbolic curve (Fig. 8) as follows:

$$P = \frac{\delta - \delta_0}{b + a(\delta - \delta_0)} \tag{2}$$

where P is the axial load, δ is the pile head deflection, δ_0 is the pile head deflection for the case of zero axial load, a and b are the curve fitting parameters (Fig. 8). As shown in the pile buckling analysis method within the widely-used commercial software LPILE (Isenhower and Wang 2014), the buckling load P_{cr} could be estimated from the shape of the pile-head response curve (Fig. 8), which is the limit value of axial load and could be computed using Equation (3).

$$P_{cr} = \frac{1}{a} \tag{3}$$

It is hard to verify this estimated method of buckling load, due to there is no test data about the buckling load of the pile in liquefied ground. So the Euler buckling load for the unsupported column, as a limit case, is used to examine the estimated method. The analysis is performed using the same parameters as Pile 2 in the experiment. For this case, the estimated buckling load P_{cr}=1.3141 kN is almost identical to the Euler buckling load of P_E=1.3138 kN, which indicates that this method is able to evaluate the buckling load of the pile.

4.3 Effect of inertial load on buckling instability

The pile head deflection versus axial load under different inertial loads is shown in Fig. 9. The estimated buckling load for the inertial load of 0.1 kN, 0.15 kN, and 0.20 kN are 2.21 kN, 1.88 kN, and 1.67 kN, respectively. It indicates that the increase in the inertial load would lead to a decrease of the buckling load of the pile because larger lateral load would lead to larger deflection of the pile thus leading to the formation of plastic hinges at a lower axial load.

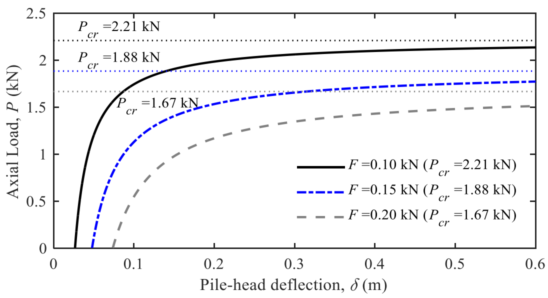

Fig. 9 Effect of inertial load on estimated buckling load

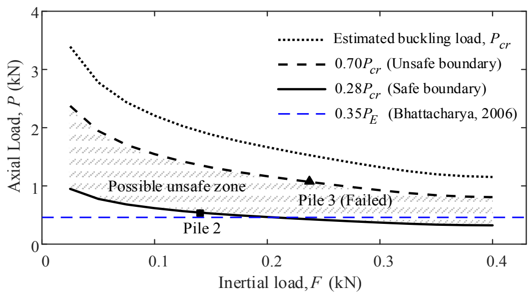

Fig. 10 Safe and unsafe boundary for buckling instability of the pile

The estimated buckling load under different inertial load is given in Fig. 10. It can be seen that the axial load of Pile 3 is smaller than the estimated buckling load. However, Pile 3 was damaged during the shaking. This is because piles are likely to have geometrical imperfections, residual stresses due to driving, stiffness deterioration during life, and eccentric load (Bhattacharya 2006). All these uncertain factors may cause the actual buckling failure load of the pile to be much lower than that predicted by Equation (4). Therefore, a conservative safe boundary (0.28P_{cr}) and a highly probable unsafe boundary (0.7P_{cr}) were suggested here based on the results of the shake-table test (Fig. 10). Additional experimental data are needed to explore the possible safety boundary further and verify if these results can be applied to other more complicated cases.

Bhattacharya (2006) suggested that the pile may not buckle if the axial load is below 0.35 times P_E which the influence of lateral load is not considered. By comparing the safe boundary proposed in this paper with that in Bhattacharya (2006), as shown in Fig. 10, it is not certain if the pile with an axial load below 0.35 times P_E will definitely not buckle if the lateral load is large enough. It is hence important for the designers to take into account the lateral load during buckling analysis of pile in liquefying ground. However, the range between the bounds of $0.28P_{cr}$ and $0.7P_{cr}$ is still very wide, further tests are needed to establish a more precise boundary of safe lateral load for a given axial load.

5. Conclusions

This study provides a better insight into the buckling instability of pile in liquefied soils. In this paper, a shake-table test and the associated pseudo-static analysis were employed to investigate the effect of lateral load on buckling failure of the pile. The main conclusions are as follows:
(1) The pile could fail in buckling mode in liquefying ground has been confirmed again by shake-table test, and the buckling instability happened after the soil has just fully liquefied.
(2) The pseudo-static analysis method based on the Beam on Nonlinear Winkler Foundation model is effective in simulating the pile response under the combined action of lateral load and axial load in liquefied soils.
(3) Pile foundations design should consider the buckling mechanism together with the effect of lateral load. An increase in lateral load will decrease the buckling load of the pile. A conservative safety boundary for avoidance of buckling failure taking into account of the influence of lateral load has been suggested.
(4) Additional experimental data, along with related numerical analyses, to further explore the influence of lateral load on buckling mechanism of the pile and to reduce the range of uncertainty of safe boundary are needed.

Acknowledgments

This work was supported by the National Natural Science Foundation of China (Grant Nos. 51578195 and 51378161). Prof. Guoxing Chen, Prof. Haiyang Zhuang, and Assoc. Prof. Li Wan at Nanjing Tech University provided much useful assistance in performing the shake-table test. This assistance and support are greatly acknowledged.

References

Abdoun, T., and Dobry, R. (2002) Evaluation of pile foundation response to lateral spreading, Soil Dynamics and Earthquake Engineering, Vol 22, No 9, pp 1051-1058.

Abdoun, T., Dobry, R., O'Rourke, T. D., et al. (2003) Pile response to lateral spreads: centrifuge modeling, Journal of Geotechnical and Geoenvironmental Engineering, Vol 129, No 10, pp 869-878.

Bhattacharya, S. (2003). Pile Instability during Earthquake Liquefaction. University of Cambridge.

Bhattacharya, S. (2006) Safety assessment of existing piled foundations in liquefiable soils against buckling instability, ISET J Earthq Technol, Vol 43, No 4, pp 133-147.

Bhattacharya, S., Bolton, M., and Madabhushi, S. (2005) A reconsideration of the safety of piled bridge foundations in liquefiable soils, Soils and Foundations, Vol 45, No 4, pp 13-25.

Bhattacharya, S., and Madabhushi, S. P. G. (2008) A critical review of methods for pile design in seismically liquefiable soils, Bulletin of Earthquake Engineering, Vol 6, No 3, pp 407-446.

Bhattacharya, S., Madabhushi, S. P. G., and Bolton, M. D. (2004) An alternative mechanism of pile failure in liquefiable deposits during earthquakes, Geotechnique, Vol 54, No 3, pp 203-213.

Boulanger, R. W., Kutter, B. L., Brandenberg, S. J., et al. (2003). Pile foundations in liquefied and laterally spreading ground during earthquakes: centrifuge experiments & analyses: Center for Geotechnical Modeling, Department of Civil and Environmental Engineering, University of California, Davis, California.

Brandenberg, S. J., Zhao, M., Boulanger, R. W., et al. (2013) p-y Plasticity Model for Nonlinear Dynamic Analysis of Piles in Liquefiable Soil, Journal of Geotechnical and Geoenvironmental Engineering, Vol 139, No 8, pp 1262-1274.

Chen, G., Zhou, E., Wang, Z., et al. (2016) Experimental investigation on fluid characteristics of medium dense saturated fine sand in pre- and post-liquefaction, Bulletin of Earthquake Engineering, Vol 14, No 8, pp 2185-2212.

Dash, S. R., Bhattacharya, S., and Blakeborough, A. (2010) Bending–buckling interaction as a failure mechanism of piles in liquefiable soils, Soil Dynamics and Earthquake Engineering, Vol 30, No 1–2, pp 32-39.

Finn, W., and Fujita, N. (2002) Piles in liquefiable soils: seismic analysis and design issues, Soil Dynamics and Earthquake Engineering, Vol 22, No 9, pp 731-742.

Haldar, S., Sivakumar Babu, G. L., and Bhattacharya, S. (2008) Buckling and bending response of slender piles in liquefiable soils during earthquakes, Geomechanics and Geoengineering, Vol 3, No 2, pp 129-143.

Isenhower, W. M., and Wang, S. (2014) User's manual for LPile 2013, Ensoft, Austin, TX, Vol, No, pp.

Ishihara, K. (1993) Liquefaction and flow failure during earthquakes, Geotechnique, Vol 43, No 3, pp 351-415.

Knappett, J. A., and Madabhushi, S. P. G. (2009) Influence of axial load on lateral pile response in liquefiable soils. Part I: physical modelling, Geotechnique, Vol 59, No 7, pp 571-581.

Mazzoni, S., McKenna, F., Scott, M. H., et al. (2006) OpenSees command language manual, Pacific Earthquake Engineering Research (PEER) Center.

Shanker, K., Basudhar, P. K., and Patra, N. R. (2007) Buckling of piles under liquefied soil conditions, Geotechnical and Geological Engineering, Vol 25, No 3, pp 303-313.

Tokimatsu, K., Oh-oka, H., Satake, K., et al. (1998). Effects of lateral ground movements on failure patterns of piles in the 1995 Hyogoken-Nambu earthquake. Paper presented at the Geotechnical Earthquake Engineering and Soil Dynamics III.

Turner, B. J., Brandenberg, S. J., and Stewart, J. P. (2016) Case Study of Parallel Bridges Affected by Liquefaction and Lateral Spreading, Journal of Geotechnical and Geoenvironmental Engineering, Vol 142, No 7, pp 05016001.